BURSTPROOF, THERMAL PRESSURE SENSOR FOR GASES

Ulrich Bonne and Dave Kubisiak

Honeywell Technology Center, 10701 Lyndale Ave.S., Bloomington, MN 55420
Voice/fax/e-mail: (612)956-4477/956-4517/bonne_ulrich@htc.honeywell.com
Voice/fax/e-mail: (612)956-4072/956-4517/dkubisiak@p01.mn09.honeywell.com

ABSTRACT

We have extended the operating range of thermal conductivity-based pressure sensors (Pirani gauges) to above 200 bar, corrected for the influence of changes in gas composition and temperature, and demonstrated repeatabilities comparable to state-of-the-art precision (±0.1%) industrial pressure sensors.

This paper describes how such on-line corrections can be made via thermal measurements with two microbridge sensors of different dimensions, so that the effect of absolute thermal conductivity changes are sensed and effectively eliminated. The required measurements include temperature, heater conditions, and steady-state and transient heat transfer. For measuring high pressures, we took advantage of the nonideal gas changes in thermal conductivity. All the above (thermal-only) measurements were performed with single, 1.7 x 1.7-mm, Si chip sensors machined fromsingle Si wafers.

INTRODUCTION

This paper describes improvements of the Pirani-type or thermal conductivity-based, absolute pressure microsensors. Despite of their attractive overpressure-proof feature, they have suffered from three major disadvantages: limitation to gaseous fluids, sensitivity to gas composition changes and operation limited to pressures below atmospheric. We describe here means to eliminate the last two by introducing an approach to compensate for composition changes and by extending the useful operating range to above 150 bar. The goal is to be able to fabricate low-cost, fully compensated (temperature, composition and pressure) gas flow sensors, for metering of domestic and compressed natural gas.

The microsensor structure is very similar to those used and reported earlier[1-3], although the conductor films are of Pt and not of NiFe[1] or polysilicon[2,3].

The challenge we faced was to derive an on-line, thermal pressure sensing means, while eliminating the influence of an unknown gas composition (and temperature), without giving up the burstproof feature, low-cost, low-power and the self-contained nature of the sensor. We first pursued a compensation that was based on sensing the volumetric, isobaric specific heat, $c_{pv} = c_p\rho$, which is closely proportional to pressure[4,5], to which a measurement of thermal conductivity, k, would be added for composition correction[5]. But we found that the compensated pressure signal was so sensitive to prime sensor signal noise as to be useless. That is when we turned to the use of two microbridge (MB) structures of different geometry, to take advantage of expected differences in pressure- (or mean-free-path-) dependent heat loss[6], as will be described below.

EXPERIMENTAL

The silicon-based, micromachined sensor chip, besides supporting the basic, narrow MB structure shown in Figs.1 and 2, also supported Wheatstone bridge reference resistors to provide for a first-order temperature compensation[7], and a wide MB structure, as used for flow measurements[7]. The bridge width and gap dimensions were about 3 μm for the former and over 100 μm for the latter. One complete chip layout is shown in Fig.3. To achieve a combination of the desired level of ruggedness and sufficient resistance with the narrow MB structure, its 10 segments of self-supported films were anchored to the substrate at intervals of about 60 μm, as shown[1]. All heater serpentines consisted of 0.1-μm

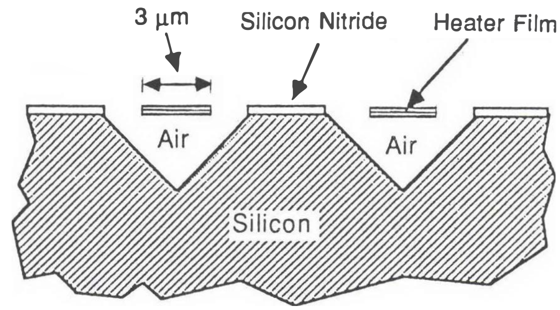

Fig. 1. Cross section of pressure microsensor[1].

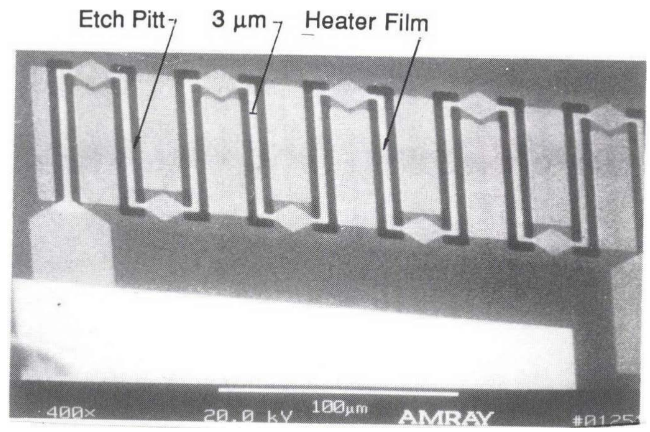

Fig. 2. SEM micrograph of thermal pressure sensor, showing narrow microbridge and gap of 3 μm.

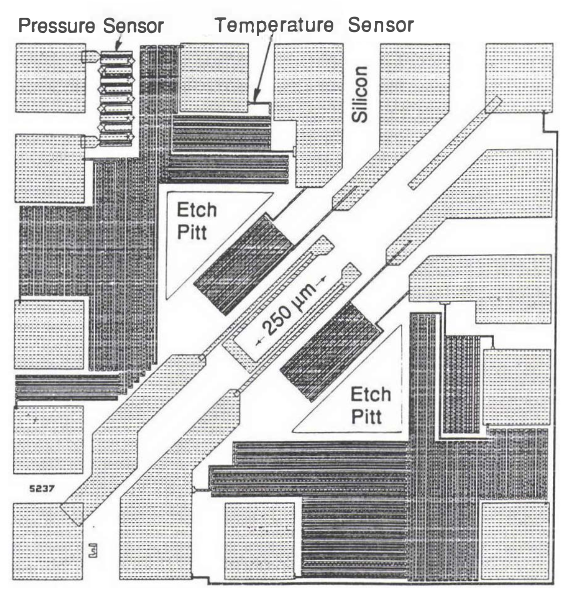

Fig. 3. Microsensor chip layout.

films of Pt, embedded in stress-reduced Si_3N_4 films of about 1-µm total thickness. The square Si chip measured 1.7 µm on the side and was mounted and Au-wire bonded to standard TO5 headers. These headers could then be fastened and doubly sealed (via a metal-metal seal and a 0.5-mm-thick O-ring) to the test chamber.

The measurement circuit of the basic pressure microsensor simply consisted of a DC Wheatstone bridge. It served to maintain the heated MB structure at a constant temperature, set between 85 and 100°C, by varying the applied potential to keep the bridge in balance, and to determine its dissipated power by sensing the heater current and voltage drop. These were then digitized and multiplied.

Mean free paths were determined via published values of effective molecular collision cross sections according to the expression[8]:

$$L = RT/(N\sqrt{2}\pi\sigma_m^2) \qquad (1)$$

where R = 80.206 atm·cm³/(Kmol), Universal Gas Constant; T = absolute temperature in K; N = $6.023 \cdot 10^{23}$/mol, Avogadro Number; and $\pi\sigma_m^2$ = molecular collision cross section, (σ–values in Å, as derived from Lennard-Jones potentials, are: 3.65 for air, 3.82 for CH_4, 3.40 for Ar and 1.9 for He[8]; better fits were obtained with 3.6 for CH_4, 3.8 for Ar and 1.45 for He and are within the range of values listed in ref.[8] for alternative methods for deriving σ-values). These cross-section data were used initially only, for evaluation of experimental data, before the use of microbridges of different geometry was adopted.

The on-line determination of k and c_{pv} was accomplished with the wide heater elements on the chip, as described earlier[4]. This method consists of processing measurements of gas tempeature and both transient and steady-state sensor temperature rise caused by heat transfer from an adjacent, intermittently heated thin-film element. Calibration of this k, c_{pv} and pressure sensor was accomplished with an automated system, which would expose the sensor to three gases, six temperatures and six pressures, and record the measured environmental conditions, the above wide MB sensor outputs and the wide and narrow MB heater conditions. This process took about 8-10 hours and could be completed overnight.

For pressure measurements above 2 bar, the above sensor package was sealed to a ≤3-cm³ stainless steel chamber that could be connected directly to the ≤200-bar gas pressure of a steel gas tank.

RESULTS AND DISCUSSION

Examples of the measured pressure dependences for both wide and narrow MBs are shown in Figs.4-6. Note that the steep rise in heat loss is well on its way at 10^{-2} bar in Figs.4 and 5 (wide MB) but not in Fig.6 (narrow MB), indicating the expected shift toward higher pressures, i.e. smaller mean free paths, as the MB dimensions are reduced. We verified that the plotted heat loss data at high pressures were directly proportional to k and that mean free path, L, and pressure, p, were "interchangeable"; i.e. that by choosing dry air as reference gas, correcting the heat loss data points acording the transformation $Q_{corr} = (Q - Q_{vac})k_{air}/k_i + Q_{vac}$, and shifting the pressure points from p to pL_{air}/L, the data of all gases collapsed into the set measured for air, see Fig.5. In other words, the experimental heat loss data at low pressure could be represented by points of heuristic eq.(2) plotted by using either (1) a L/L_{air} pressure scale shift and setting all $L_i \equiv L_{air}$, or (2) no pressure scale shift and letting L_i represent individual mean free paths. In both cases, the k_i represent the k-values of gases "i":

$$Q = Q_{vac} + k_i/k_{air}\{A_1\exp(-A_2/p/L_i) + A_3\exp(-[A_4/p/L_i]^{0.5})\} \qquad (2)$$

with the constants Q_{vac} = 0.33 mW is the measured residual heat loss in vacuum, k_{air} = 68.255 µcal/(cmKs), A_1 = 0.64998, A_2 = $1.291638 \cdot 10^{-6}$ psi·cm, A_3 = 0.65996, and A_4 = $2.741976 \cdot 10^{-7}$ psi·cm. The only variables are k_i = thermal conductivity of gas "i" in µcal/(cmKs), L_i = its mean free path in cm and p = pressure in

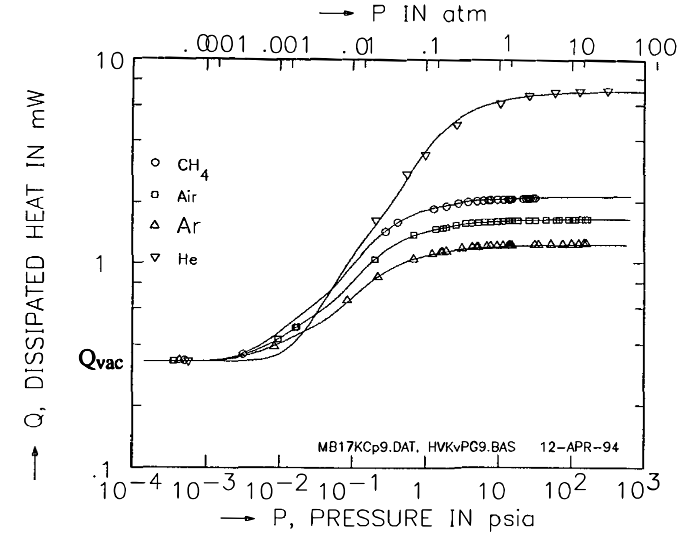

Fig. 4. Heat dissipated by a wide MB pressure sensor heater, for four gases. Data without composition correction. The fitted functions are of the form: $Q = Q_{vac} + k_i/k_{air}\{A_1\exp(-A_2/p/L_i) + A_3\exp(-[A_4/p/L_i]^{0.5})\}$

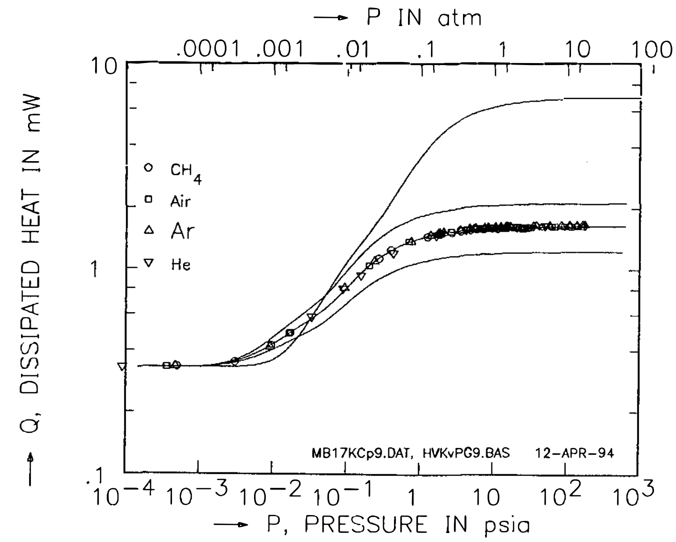

Fig. 5. Heat dissipated by a wide MB pressure sensor heater, for four gases. Data after composition correction.

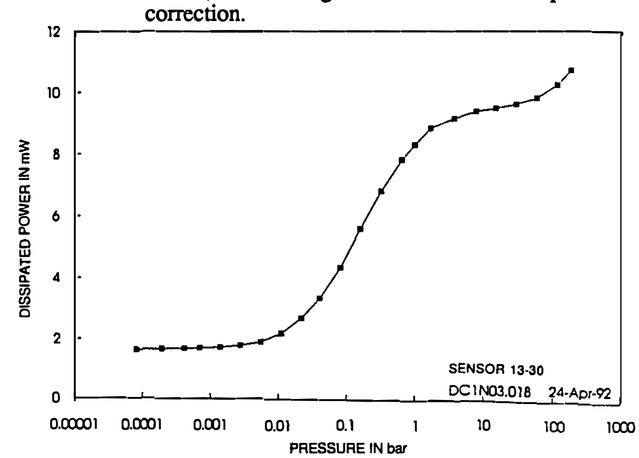

Fig. 6. Heat dissipated by a Pirani-type, narrow MB pressure sensor, up to high pressures. Sensor 13-30 before linearization, in nitrogen.

psia. In eq.(2) the k_i thus define the heat loss at high pressure and the L_i the transition region from the Q_{vac}. The second exponential term was needed to improve the quality of the curve fits, which was not deemed surprising in view of the odd geometry of the narrow MB.

The determination of effective L(σ)-values that led to the best fits of Q(p), as described in the Experimental section, is offered as a (possibly new?) tool for probing into the combined influences of molecular cross section and thermal accommodation at gas-solid interfaces, involving transfer of kinetic, rotational and/of vibrational energy[9]. However, in spite of the encouragment provided by the gained physical understanding, we still needed a method for on-line, self-contained determination of mean free path, if this pressure sensing approach was to be practical. But rather than search for a method to determine L, in view of the range of uncertainty presented for its values in ref.[8], we decided to first lump all available data into one fitted expression for presure, p, and then interpret the physics of the findings later, if warranted. The chosen expression has the form of a polynomial:

$$p = f(k, c_{pv}, I_H, V_H, I_h, V_h, T) \quad (3)$$

where I and V = heater current and voltage, respectively, and the subsripts H and h refer to the wide and narrow MBs[6]. No effort was made at the time to determine if all the listed independent variables were needed, an effort that may indeed improve the quality of the fit.

Figs.7 and 8 show examples of results obtained with this method. They were plotted after a calibration run, as described in the Experimental section, and show that the composition-dependence can be eliminated, while achieving pressure measurements to within an uncertainty of less than ±1%, see Fig.7. A near-term repeatability of better than ±0.2% is shown in Fig.8. In both figures the thermal pressure sensor is compared with an industrial-grade, precision, Si-piezoresistive pressure sensor (Honeywell ST3000). Fig.8 also shows that the single largest contribution to pressure signal error is the noise of the c_{pv} signal; to avoid small (0.1-0.5%) but systematic errors due to thermal convection effects, we recommend that the sensor not be used in orientations different from the one set during calibration, or that means be provided to compensate for the effect of such convective flows.

Regarding operation at high pressures, Fig.6 shows that the chosen narrow MB geometry has shifted the end of the mean free path-dependent heat loss rise to pressures that are high enough to allow the observation and utilization of the beginning of the increase in k-values due to the increasingly non-linear behaviour of gases. For example, Figs. 9 and 10 show the effects of nonideal (i.e.pressure-dependent) behavior of methane[4], which give the appearance of steadily increasing values of k and c_p above 10 bar. That is reflected in the renewed rise in heat loss above that pressure in Fig.6.

A remaining challenge is to extend the composition (and temperature) correction to those higher pressures, as illustrated in Fig.11 for CH_4, C_2H_6 and N_2, for 300 and 350 K, using simple thermal conductivity functions of the type

$$k(T,p) = a_1 + a_2T^{n_1} + a_3T^{n_2}p^{n_3} \quad (4)$$

which were also used to represent the property data by Vargaftik[10] plotted in Figs.9 and 10. Note that the data plotted in Fig.9-11 did not take mean-free-path effects into account, but that Fig.9 shows that eq.(3) successfully compensated for the influences of both L and T; the magnitude of the approx. $k \sim T^{0.7}$ influence is illustrated in Fig.11 by plotting curve sets for both 300 and 350 K. Another challenge is to demonstrate satisfactory stability and service life, especially at the elevated temperatures many applications require[11,12].

CONCLUSIONS AND RECOMMENDATIONS

We have demonstrated, to our knowledge for the first time, that the

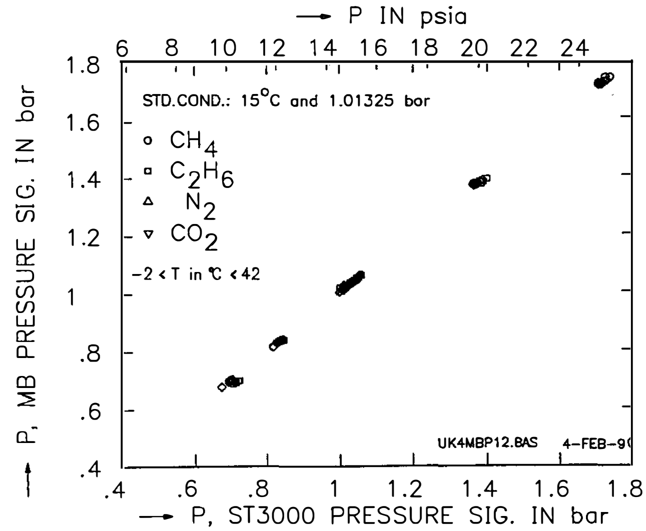

Fig. 7. Comparison between a narrow MB thermal sensor and a precision, Si-piezoresistive, industrial-grade pressure sensor.

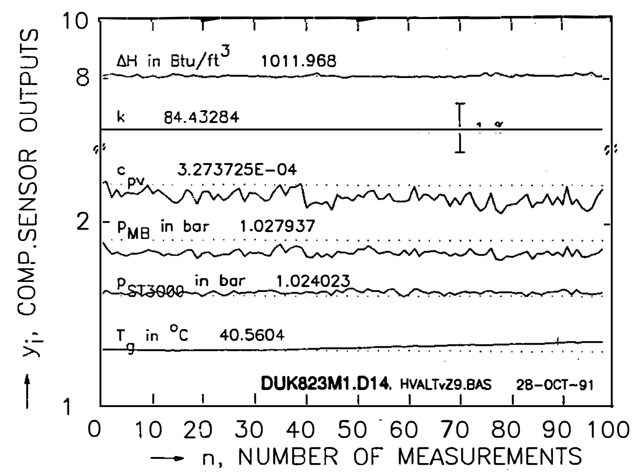

Fig. 8. Short-term repeatability of thermal pressure sensor measurements, including its compensated output, compared to a Si-piezoresistive sensor and to additional MB outputs, for methane; y-scale: 20x.

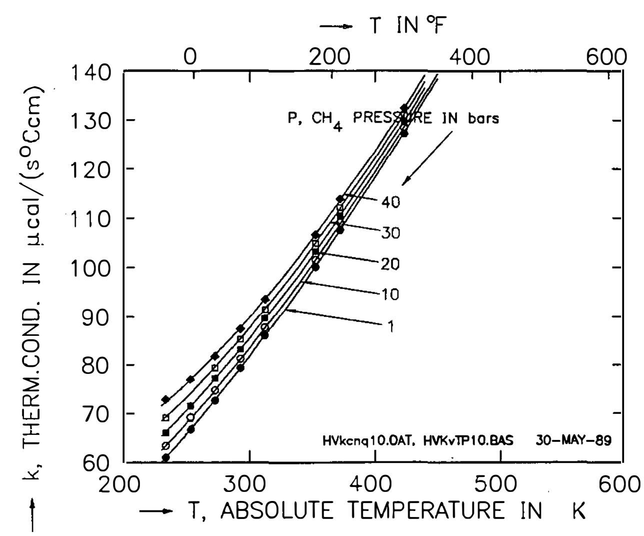

Fig. 9. Thermal conductivity of methane vs. temperature and pressure.

signals of Pirani pressure sensors can be compensated for changes in gas composition and gas temperature and that such on-line corrections can be made via measurements with two microbridge sensors of different dimensions, so that the effects of absolute thermal conductivity changes are sensed and effectively eliminated, provided that temperature and the characteristics of both heaters are also sensed.

Furthermore, increases in thermal conductivity because of the increasingly nonideal behavior of gases above atmospheric pressure were shown to provide a vehicle to extend the useful gas pressure sensing range to 200 bar and beyond.

All the above thermal-only, primary and corrective measurements were performed with single, 1.7 x 1.7-mm sensor chips machined from single Si wafers.

Future work will focus on overall signal noise reduction, reliability and service life improvements, searching for analytical replacements of the fitted, eq.(2)-type functions, and composition correction methods for use at high pressures.

ACKNOWLEDGEMENTS

We thank J.Ridley, R.Higashi, E.Satren and K.Nguyen of HTC for their help with the microsensor fabrication, evaluation and calibration, and E.Swiatkiewicz with the experimental setup. S.James generated some of the early MB heat loss data[13].

REFERENCES

1. S.D.James, R.G.Johnson and R.E.Higashi, "A Broad-Range, Absolute Pressure Microsensor," IEEE Solid-State Sensor and Actuator Workshop, Hilton Head, SC, 6-9 June 1988, Book of Abstracts, p.107
2. C.H.Mastrangelo and R.S.Muller, "μ-Pirani Pressure Gauge with Digital Readout," IEEE Tranducers '91, Int'l Conf. on Solid-State Sensors and Actuators, San Francisco, CA, 24-27 June 1991, Proceedings, p.245
3. Priti Pal S.Juneja and Glenn H.Chapman, "A Wide-Range Vacuum Sensor Employing Phase-Sensitive Detection," Canadian Conf. on VLSI (CCVLSI), Banff, Alberta, Canada, 14-16 Nov.1993, Proceedings, p.3A7
4. U.Bonne, "Fully Compensated Flow Microsensor for Electronic Gas Metering," 1992 Int'l.Gas Research Conf., Orlando, FL, 16-19 Nov.1992, Proceedings, Vol.III, p.859
5. U.Bonne, "Versatile, Overpressure Proof, Absolute Pressure Sensor," U.S. Pat. 5,187,674, 16 Feb.1993, assigned to Honeywell
6. U.Bonne, "Absolute Pressure Sensor and Method," US Pat. 5,303,167, 12 April 1994, assigned to Honeywell.
7. P.J.Bohrer, R.E.Higashi, G.B.Hocker and R.G.Johnson, "A Microtranducer for Air Flow and Differential Pressure Sensing Applications," Workshop on Micromachining and Micropackaging of Transducers, Case Western Reserve University, Cleveland, OH, 7-9 Nov. 1984, Proceedings
8. J.O.Hirschfelder, C.F.Curtiss and R.B.Bird, "Molecular Theory of Gases and Liquids," J.Wiley & Sons, Inc., 3rd Ed., (1966) pp. 10 and 552-561
9. W.A.Wakeham, Imperial College Thermophysical Properties Data Center, London, UK, Private Communication, Apr.1994
10. N.B.Vargaftik, "Hanbbook of Physical Properties of Liquids and Gases," Hemisphere Publ. Co., 1975
11. U.Bonne, "Thermal Microsensors for Environmental and Industrial Controls," (invited paper) NIST Workshop on Gas Sensors: Strategies for Future Technology, Gaithersburg, MD, 8-9 September 1993, Proceedings, to be published
12. U.Bonne and D.Kubisiak, "Determination of Compressibility Factor and Critical Compression Ratio with Si-Based Microstructure Sensors," 7th IGT Symposium on Natural Gas Quality, Chicago, IL, 12-14 July 1993, Proceedings
13. U.Bonne and S.James, "Method and Apparatus for Measuring the Density of Fluids," U.S. Pat. 4,956,793, 11 Sep. 1990, assigned to Honeywell

PBSSSA94.W01'15Apr/Pressure .76%

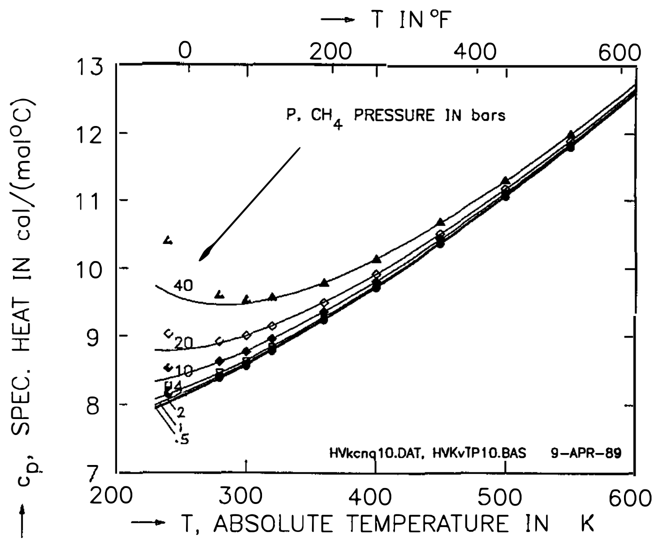

Fig.10. Specific heat of methane vs. temperature **and** pressure.

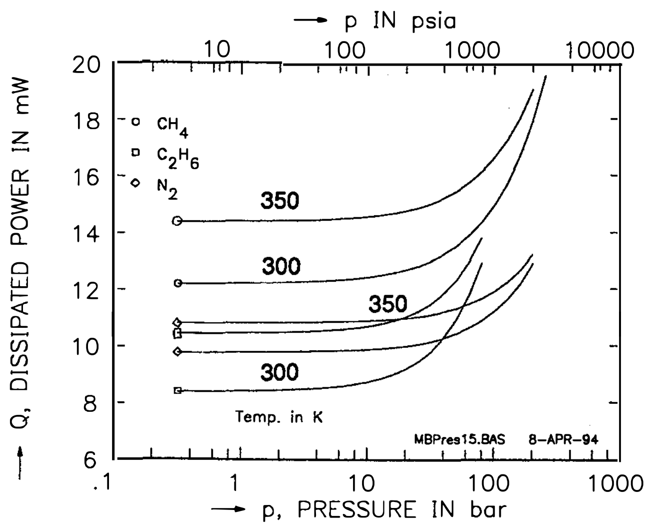

Fig.11. Calculated heat loss from a narrow MB sensor, at high pressures, for the shown gases and temperatures.